CHAPTER 2

Literature review

There are numerous materials now that can be employed in the field of supercapacitors to efficiently store energy. To meet the demands of storage devices and make them practically feasible in daily life, researchers have been working diligently and continuously. Supercapacitor electrodes are made from a variety of carbon-based materials, including graphene, activated carbon, carbon nanotubes, acetylene black, conducting polymers including polyaniline, polypyrrole, and polythiophene, and metal oxides like CuO, RuO_2, NiO, $CoFe_2O_4$, $NiFe_2O_4$, etc.[47].

2.1. Carbon-based materials

Graphene, carbon nanotubes, acetylene black, activated carbon, and other carbon-based materials are employed as supercapacitor electrodes. These materials display increased power density because they have a good surface area and are naturally conductive. It is important to note that the formation of electrodes involve the use of carbon conductive fillers [21]. They aid to increase the specific capacitance, energy, and power density and minimize internal resistance by forming conducting networks. However, using too much carbon-based material results in the agglomeration and an increase in contact resistance, which reduces conductivity. In order to satisfy both requirements, one effective carbon conductive filler can be utilized in place of both carbon-based materials and carbon conductive filler in supercapacitor electrodes [24].

2.1.1. Graphene

In today's advanced material world, besides conventional carbon-based materials, graphene and its family (graphene oxide (GO) and reduced graphene oxide (rGO)) have attracted prominent regard on account of its magnificent chemical, physical, electronic, optical and

thermal properties. Properties such as higher chemical stability, quick reactive nature, larger area (~2600 m^2 g^{-1}), a high value of young's modulus (~1 TPa), greater mobility of electron (~230,000 cm^2 V^{-1} s^{-1}), higher transparency (~95%) of incident radiation and super thermal conductivity (~3,000 W m^{-1} K^{-1}) at atmospheric conditions have convinced researchers to explore its usage in the field of supercapacitor [10,48,49]. Graphene is a two-dimensional covalently bonded carbon atoms sheet containing sp^2 hybridization. It is obtained from graphite which contains many layers of graphene (figure 2.1) and is arranged in a chicken wire hexagonal pattern which gives a perfect crystalline structure resulting in the strongest material beyond others materials. All these factors ensure that graphene is a play-field for researchers, especially in energy storage applications [50].

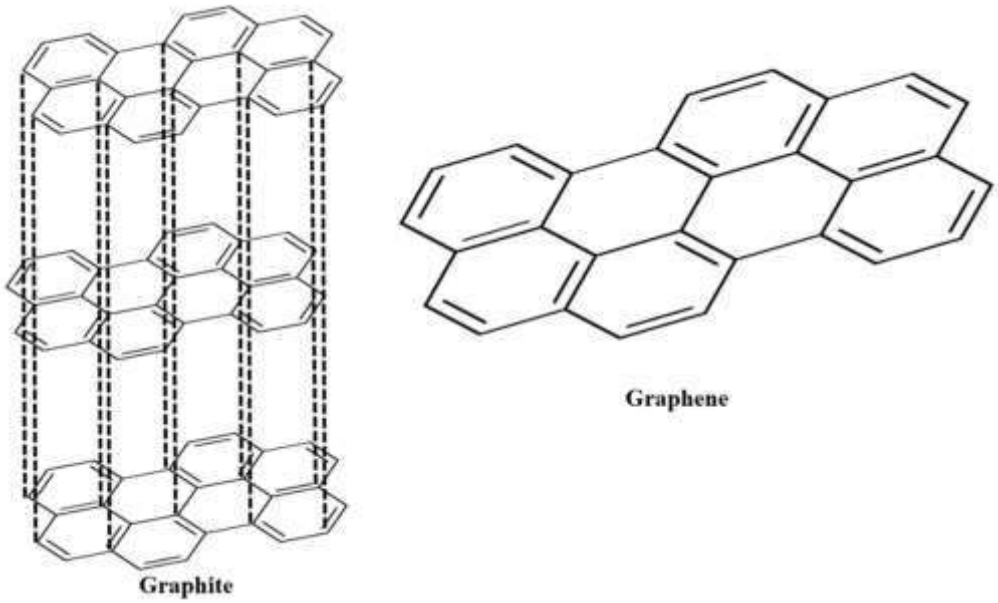

Figure 2.1: Schematic structure representation of Graphite and Graphene

The existence of free electrons in graphene make the conducting capability very high like a relativistic particle. The zero-band gap of pristine graphene ensures that it behaves like a

more metallic or semiconducting characteristic. The more metallic character shown due to their sheet sizes lies between microns to several nanometers. When the dimensions of the graphene layer are quite narrow around, 1-2 nm, it generates a separate bandgap to exhibit semiconducting properties [51]. The presence of these factors such as increasing the need for energy, fewer resources availability, and highly processing cost requires novel energy storage devices like supercapacitors, capacitors, fuel cells, solar cells and batteries discoveries. Among all, supercapacitors pay much attention because of their rapid charging rate, magnificent power density and longer stability [52].

2.1.2. Graphene structure

The sixth element of periodic table (i.e. carbon atom) has six proton-neutron in nucleus. The outer shell of carbon atom has six electrons, in which two in K class followed by four valence electrons in L class (figure 2.2 (a)). These four valence electrons in valence shell can be responsible for sp, sp^2 and sp^3 hybridization. Figure 2.2 (b) displayed the formation of sp^2 hybrids. The layered hexagonal planar formed if sp^2 hybrid carbon atoms take part with others neighboring three carbon atoms. This layered honeycomb planar called monolayer graphite or graphene. The electronic configuration of carbon is $1s^2 2s^2 2p_x^1 2p_y^1 2p_z^0$ in ground state but when 2s orbit gets sufficient energy then it's one electron jumped into $2p_z$ orbit. Due to this, $2p_z$ gets higher energy level than $2p_x$, $2p_y$ and 2s orbit reach the energy level equal to $2p_x$ and $2p_y$. So orbit 2s, $2p_x$ and $2p_y$ form the sp^2 hybridization in figure 2.2 (c). Figure 2.2 (d) illustrated that the strong σ bond form when two similar carbon atoms overlapped with two sp^2 orbitals and un-hybridized $2p_z$ orbitals overlap with another neighboring $2p_z$ orbitals responsible for formation of π bond. Generally structural integrity

is due to σ-bond and measurement of optical and electronic properties due to π-bond in graphene structure [53].

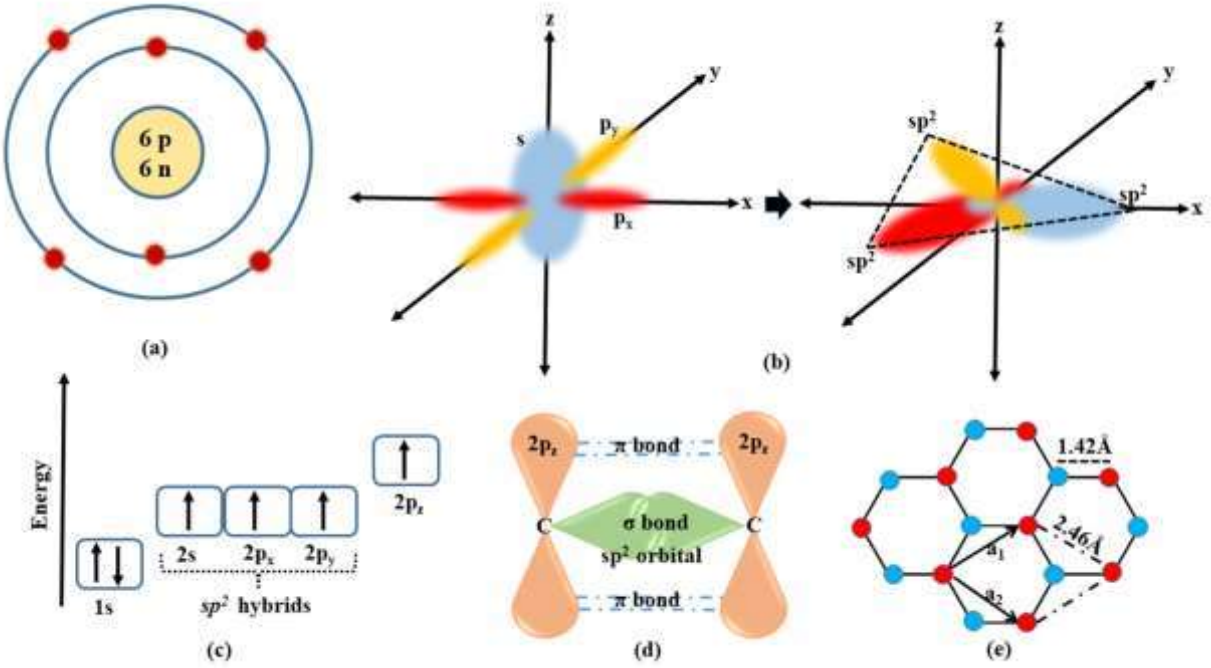

Figure 2.2: (a) Carbon atomic structure. (b) sp^2 hybrid orbitals formation. (c) Energy level of carbon atoms. (d) sp^2 hybridized σ and π bond formation. (e) Crystal lattice structure of graphene

The crystal lattice of graphene highlighted by parallelogram marked with black dark and dotted line in figure 2.2 (e). The two-unit cell vectors a_1 and a_2 with carbon-carbon spacing 1.42 Å and lattice constant 2.46 Å also represented in figure. The delocalization and resonance of electrons in π-orbitals, responsible for their extraordinary electrical properties and stability of the planar sheet [54].

2.1.3. Graphene derivatization

2.1.3.1. GO

It is a single layered carbon atoms material with different functional groups like hydroxyl, carboxylic, epoxy and ketone (figure 2.3). The presence these functional groups, GO exhibit dispersible nature in water and other solvents. This hydrophilic nature responsible for enhancing the d-spacing from 0.335 mm for graphite to 0.979 mm for GO [55]. The presence of many chemical functionalities in GO surface makes flexible chemical workplace for graphene-based nanomaterials in energy storage applications. There are various methods for GO synthesis such as Brodie, Staudenmaier, hummers, modified hummers and improved hummers with some variations to get better oxidation product economically [56–58].

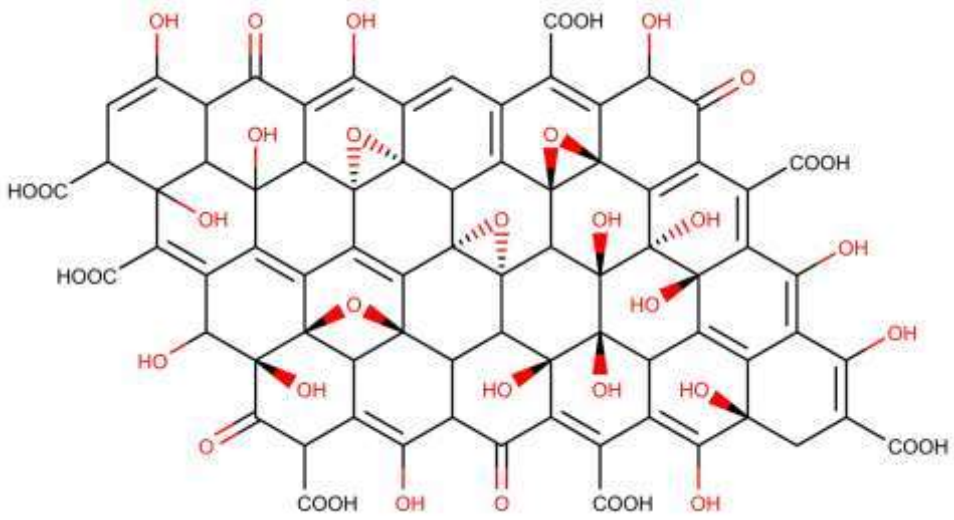

Figure 2.3: Structure model of GO

2.1.3.2. rGO

It is reduced form of GO normally denoted as rGO (figure 2.4). rGO lies between graphene and GO because of restoring graphene like properties like larger area and excellent electrical conductivity [59]. From a practical point of view, rGO cannot be considered ideal graphene but it's not false to say "real Graphene". The degree of reduction is responsible for good quality, less interlayer spacing and effective properties of rGO. There are various reduction

methods such as green methods, chemical methods, thermal methods and electrochemical methods which use different reducing agents [60,61]. Due to its incredible properties like graphene and ease of synthesis, rGO pays much attention towards energy storage devices.

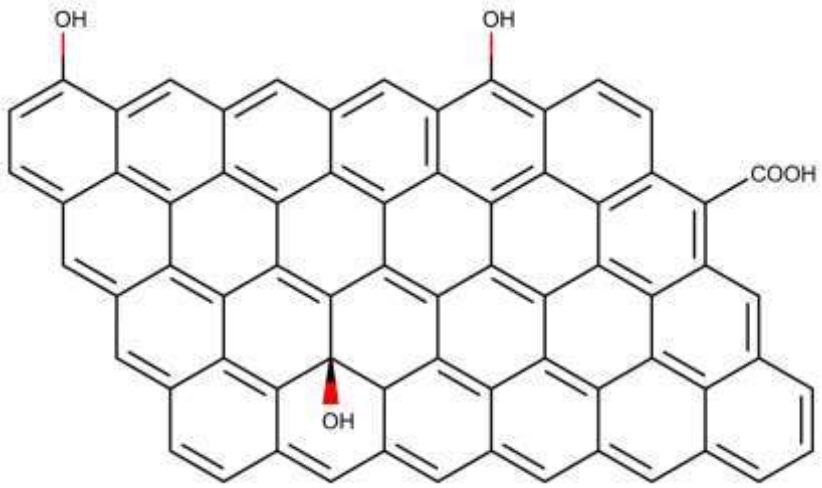

Figure 2.4: Structure model of rGO

Saito et al. (2020) synthesized graphene nanoribbons (GNRs) from chemically reduced graphene oxide with different reduction times [62]. The disorderly structure of the GNR electrode has shown a high energy density of 5.54 Wh/kg at 313 kW/kg power density and 71% capacitance retention at 100 A/g. Zhou and co-workers (2019) fabricated laser-induced bi-metallic sulfide on graphene (MoS_2/MnS/GR) nanoribbon for high performance of supercapacitors and having a high areal energy density of 7 μWh/cm^2 at 50 μA/cm^2 with 93.6% capacitance retention up to 10,000 cycles [63]. Moreover, Ujjain et al. (2015) prepared graphene nanoribbons wrapped with cobalt manganite particles for high-performance flexible supercapacitors [64]. The synergic effect of pseudo and EDLCs showed a high energy density of 44.6 Wh/kg and 11.3 kW/kg power density with 95% retention after 10,000 loops. Similarly, Ping et al. (2017) developed an Edge-riched graphene

nanoribbon by longitudinal unzipping of carbon nanotubes and displayed a larger capacitance of 202 F/g compared to GO and MWCNTs at a scan rate of 5 mV/s [65].

Li et al. (2011) synthesized graphene nanosheets with KOH activation and showed a specific capacitance of 136 F/g, which was 35% higher than pristine graphene nanosheets [66]. While, Thirumal et al. (2016) prepared boron-doped graphene nanosheets using boric acid as a boron source through a hydrothermal approach and displayed 113 F/g at 1 A/g current density when atomic doping was 2.56% [67]. Fan and co-workers (2012), synthesized porous graphene nanosheets (PGNs) by the etching over graphene sheets by MnO_2 and showed the highest capacitance of 154 F/g at 500 mV/s after etching in 6M KOH aqueous electrolyte, and obtained 88% capacitance retention after 5000 cycles [68]. Moreover, Cerium oxide is another type of metal oxide for supercapacitors because of its eco-friendly nature, economic and energetically redox actions, reported by Chakrabarty and co-workers (2021) [69]. They have developed a CeO_2/Ce_2O_3-rGO nanocomposite hybrid with different weight fractions of rGO named CRGO1 (3 wt% rGO), CRGO2 (4.5 wt% rGO), CRGO3 (7 wt% rGO), CRGO4 (9 wt% rGO), and got higher specific capacitance of 1027 F/g at 1 A/g for CRGO3 while having 90% initial capacitance retention after 1000 cycles using 1M NaOH electrolyte.

Few works have been done without using conductive fillers during the electrode fabrication process. However, replacing carbon-based materials like activated carbon, acetylene black, and carbon nanotubes with conductive fillers like graphene oxide will be cost-effective and can fulfill dual purposes (constituent and conductive filler). Table 2.1 represents the compilation of supercapacitor electrodes based on graphene materials.

Table 2.1: Electrochemical properties of various graphene based materials

Materials	C_{sp} (F/g)	Scan rate or Current density	E_{sp} (Wh/ kg)	P_{sp} (W/ kg)	Cycle life	Ref.
RGO	19.5 (3E)	1 A/g	-	-	-	[70]
3D-RGO	88.9 (3E)	1 A/g	-	-	85% @1000 cycles	[70]
MWCNT	21 (SC)	0.5 A/g	2.7	-	99% @1000 cycles	[71]
RGO	41.5 (3E)	0.1 A/g	5.8	2200	-	[72]
Graphene film	55.3 (3E)	1 mV/s	-	-	-	[73]
TRGO	75 (3E)	0.1 A/g	-	-	81% @2000 cycles	[74]
N-TRGO	82 (3E)	0.1 A/g	-	-	84% @2000 cycles	[74]
N/P-TRGO	165 (3E)	0.1 A/g	-	-		[74]

					91% @2000 cycles	
ACC	8.8 mFg^{-1} (SC)	10 mV/s	-	-	95% @20000 cycles	[75]
RGO/CNT	47 (SSC)	0.1 A/g	4.2	61.7	-	[76]
RGO	80 (3E)	2 mV/s	-	-	-	[77]
RGO@CS	200 (3E)	2 mV/s	7	-	-	[77]
RGO	173.4 (3E)	1 A/g	6.5	500	85.6% @10000 cycles	[78]
Graphene hydrogel	186 (SC)	1 A/g	0.12	460	91.6% @10000 cycles	[79]
Graphene	245 (SC)	1 A/g	8.01	5970	83% @10000 cycles	[80]
Graphene fiber	179 (SC)	0.2 A/g	5.76	47.3	-	[81]

TRGO = Thermally reduced graphene oxide

N/P-TRGO = Nitrogen/phosphorous codoped thermally reduced graphene oxide

ACC = Activated carbon cloth

SC = Supercapacitor

2.2. Conducting polymers

Various conducting polymers have been synthesized to attain excellent electrochemical properties. The chemical structures of commonly adapted conducting polymers are shown in figure 2.5 [82,83]. The electronic nature of conducting polymers arises due to the presence of delocalized π electrons. The atom spreads over a wide range of the conjugated polymeric structure when its backbone has planar molecular structure. The salient features of delocalized π (pie) electron conjugated polymer systems, which differentiate them from conventional polymers having σ (sigma) bonds, are (i) small electronic band gap of approximately 1-3.5 eV, (ii) ease of doping-dedoping and oxidation-reduction, (iii) charge mobilities in the polymer backbone [84,85].

Among all the existing conducting conjugated polymers, polyaniline has caught the attention and is extensively used for energy storage purpose due to the following reasons [86].

(a) Excellent environmental and chemical stability.

(b) Controlled electrical conductivity.

(c) Excellent yield from the polymerization of monomers.

(d) Inexpensiveness of aniline monomer (pyrrole and thiophene are very costly).

(e) Easy synthesis.

(f) Mechanical flexibility.

(g) Simple doping by protonic acid.

(h) Out of all the conducting polymers, PANI is the only conjugated polymer whose electronic structure and electrical conductivity can be optimized by both protonation and chemical oxidation.

(i) The nitrogen atom present in PANI occupies the quinoid and benzenoid rings in the polymeric backbone and plays a vital role in the formation of π bond and interchain electrical conduction. Such type of conjugation is different from polypyrrole, as the heteromolecules in polypyrrole do not contribute in developing π bonds.

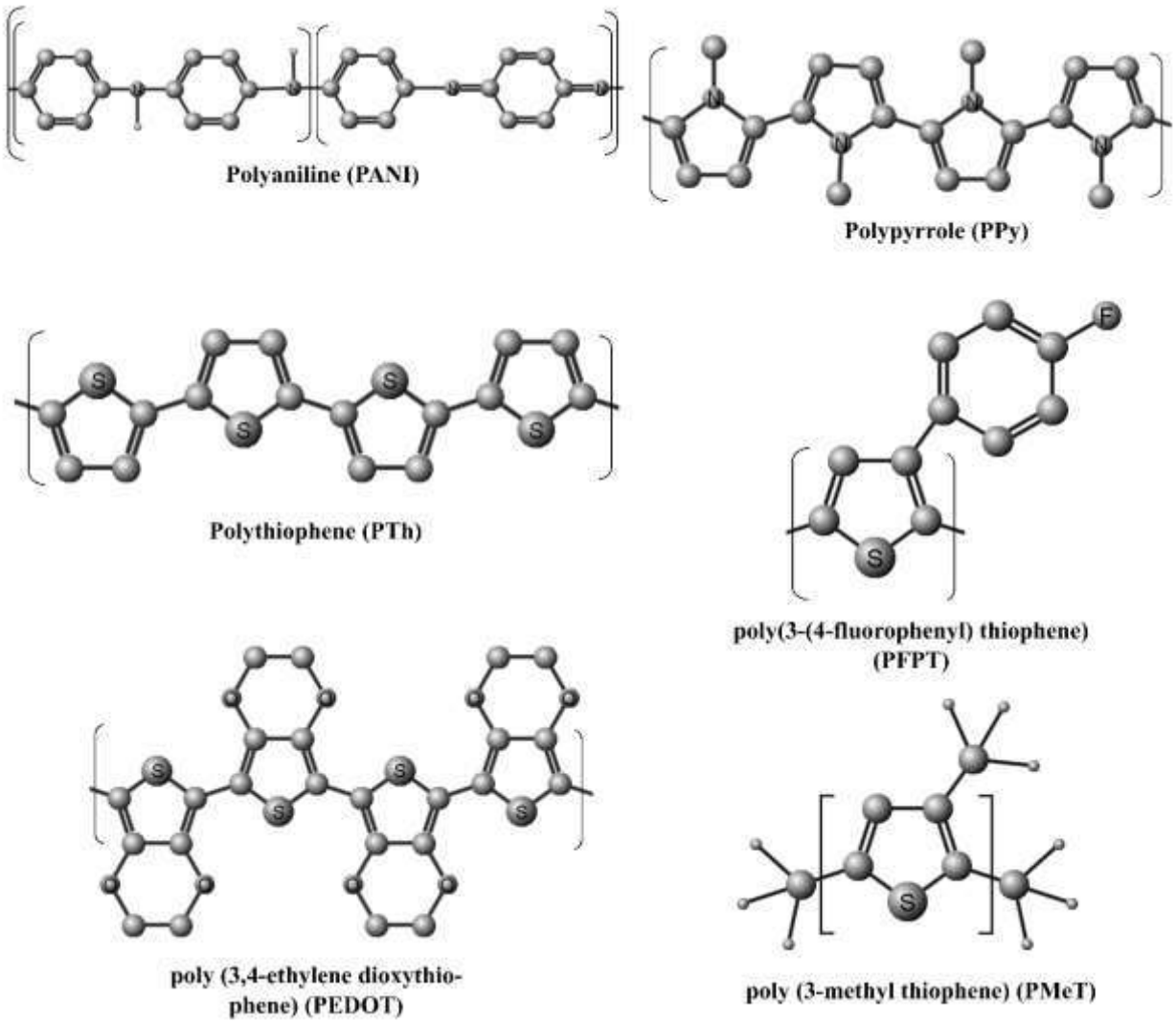

Figure 2.5: Different types of conducting polymers

2.2.1. PANI

PANI has various forms, which differ in physical and chemical properties. The conducting nature of PANI is generated by doping proper dopant and creating various oxidized and reduced states. The main four oxidation states of PANI are leucoemeraldine base (LB), emeraldine salt (ES), and pernigraniline base (PB) [87]. Figure 2.6 displays various states of polyaniline.

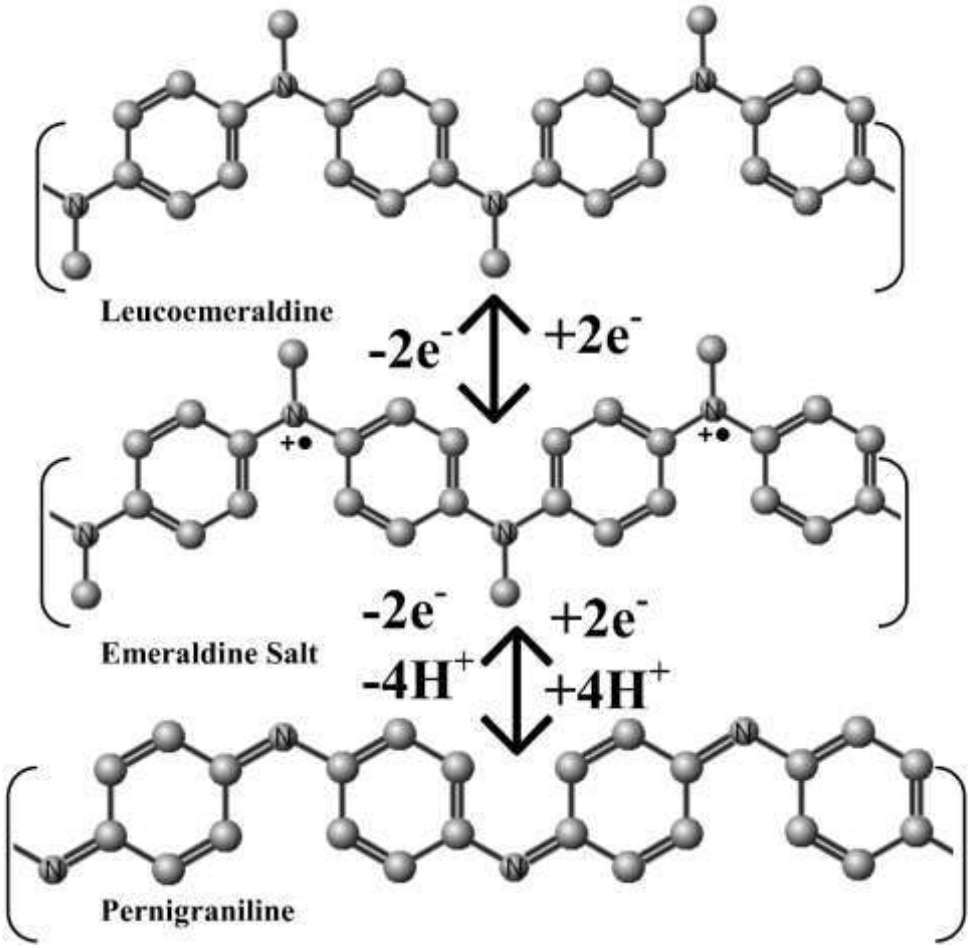

Figure 2.6: Different states of PANI

Among all the states, ES is highly conducting in nature. ES is obtained by protonating emeraldine base with the help of a suitable protonic acid. This doping process is non-redox

in nature. Redox doping of LB and PB could provide conducting ES. Both, the redox and non-redox doping processes are reversible [88]. The most common, efficient, simple and cost-effective synthesis technique of PANI is COP as polymerization and doping take place simultaneously. In COP process, an acid is used as a dopant and an oxidizing agent is used to excel (as initiator) the oxidative polymerization process. The oxidizing agent (oxidant) withdraws a proton from the aniline molecule and creates defects. Optimum amount of oxidant must be used to avoid oxidative deterioration of PANI [89]. Various dopants and oxidants are used for the synthesis of polyaniline by oxidative polymerization reactions. The most common dopants are HCl, H_2SO_4, DBSA (dodecyl benzene sulfonic acid), CSA (camphorsulfonic acid), etc. while the common oxidants are $FeCl_3$, $AgNO_3$, $K_2Cr_2O_7$, APS, etc. The use of proper dopant and oxidant can help in forming conducting polyaniline with excellent electrochemical properties [90].

Yanan et al. (2019) fabricated PANI/CCNs based symmetric supercapacitors, which gave a specific capacitance of 72 F/g at 0.1 A/g along with a power and energy density of 85.1 W/kg and 28.9 Wh/kg [91]. They used HCl as dopant and APS as oxidant during the synthesis process, and obtained agglomerated PANI particles. Chang et al. (2002) studied the effect of polymerization temperature (4°C to 50°C) on the electrochemical properties [92]. Polyaniline synthesized at lower temperature exhibited better electrochemical performances due to lower and higher degree of defects and doping, respectively. They found that 4°C was the optimized polymerization temperature. Rong et al. (2019) synthesized MoS_2-NH_2/PANI nanosheets with excellent specific capacitance of 326.4 F/g at 0.5 A/g [93]. They varied the amount of aniline as 100, 150, 200, and 300 µL in the composite and found that aniline content with 150 µL exhibited the best electrochemical properties with energy and power

density of 4 Wh/kg and 175 W/kg. They used HCl and APS (APS:aniline = 1:1.5) for the synthesis of PANI and got irregular, agglomerated structures. Fatin et al. (2017) synthesized polyaniline by taking APS and HCl as oxidant and dopant, respectively [94]. They synthesized nanocomposite of PANI-$ZnCo_2O_4$ by blending PANI and $ZnCo_2O_4$ in the weight ratio of 5:1. Interconnected tubular polyaniline particles were obtained and the presence of polyaniline helped in avoiding the agglomeration of $ZnCo_2O_4$. The binary composite and activated carbon based asymmetric device reached a maximum power density of 2997 W/kg at an energy density of 8 Wh/kg. Jiayi et al. (2019) developed a ternary composite of PANI-MnO_2-carbon nanofiber-based system [95]. Nanowires of PANI was obtained by using H_3PO_4 as dopant and APS as oxidant during the oxidative polymerization reaction. Symmetric supercapacitor of PANI/MnO_2/carbon nanofiber exhibited a specific capacitance of 342.5 F/g at 0.5 A/g along with specific energy and power of 23.3 Wh/kg and 174.9 W/kg, respectively. Manas et al. (2014) synthesized $CoMoO_4 \cdot 0.75H_2O$/PANI composite by adding $CoMoO_4 \cdot 0.75H_2O$ into aniline-APS solution during oxidative polymerization reaction [96]. The morphology of polyaniline resembled sphere shapes. The composite based device had a specific capacitance of 380 F/g at 1 A/g along with energy and power density of 42.7 Wh/kg and 450 W/kg, respectively. Jianpeng et al. (2019) took $HClO_4$ as dopant and APS as oxidant to synthesize graphene/polyaniline nanofibers [97]. They obtained a specific capacitance of 135 F/g at 1 A/g for graphene/polyaniline based asymmetric supercapacitor along with energy and power density of 18.8 Wh/kg and 1000 W/kg, respectively. Maqsood et al. (2020) fabricated polyaniline nanofibers by electrodepositing aniline-H_2SO_4 solution on flexible stainless-steel substrate [98]. The symmetric device exhibited 473 F/g of specific capacitance at 5 mV/s along with specific power and energy of 667 W/kg and 22 Wh/kg, respectively.

Murat et al. (2015) prepared PANI/CuO, PPY/CuO, PEDOT/CuO based systems, and the obtained specific capacitances at 5 mV/s were 276.56 F/g, 20.78 F/g, 198.89 F/g, respectively [99]. After 500 cycles, PANI/CuO, PPY/CuO, PEDOT/CuO based composites exhibited capacitance retentions of 81.82%, 48.39%, 68.55%, respectively. Yanmin et al. (2020) synthesized polyaniline nanofibers by taking 4-Dodecylbenzene sulfonic acid (DBSA) as a dopant and APS as an oxidant and obtained a specific capacitance of 146 F/g [100]. Xueyan et al. (2018) in their research concluded that using APS as an oxidant to prepare PANI/GNP based electrochemical system resulted in higher yield of polyaniline and hence higher pseudocapacitance in comparison to $FeCl_3$ oxidant [101]. The degradation of electrochemical activity could be due to the over oxidation of polyaniline when $FeCl_3$ was used. A systematic compilation of the work done with PANI/PANI-composite has been given in table 2.2.

Table 2.2: Electrochemical properties of polyaniline based supercapacitor electrodes and devices

Materials	PANI Shape	Technique	Dopant	Oxidant	C_{sp} (F/g)	Scan rate or Current density	E_{sp} (Wh/kg)	P_{sp} (W/kg)	Cycle life	Ref.
PANI	Nanobelt	COP	HCl	APS	304.4 (3E)	0.5 A/g	-	-	40.65% @1000 cycles	[102]
PANI	Nanotubes	COP	Benzene tetracarboxylic acid	APS	107 (SSC)	0.2 A/g	9.5	80	90.9 % @5000 cycles	[103]

PANI	PANI	PANI@TiO_2/ $Ti_3C_2T_X$	PANI/CNF	PANI/SWCNT	PANI	PANI	PANI
Nanorods	Layered flowers	Nanoflakes	Nanofibers	Nanofibers	Nano nest	Nanowires	Nanofiber
COP	COP	COP	COP	IP	EP	EP	EP
H_2SO_4	HCl	HCl	HCl	CSA	H_2SO_4	$HClO_4$	-
APS	APS	APS	APS	-	-	-	-
455.1 (3E)	272 (3E)	188.3 (3E)	234 (3E)	355 (3E)	757 (3E)	373.6 (3E)	320 (3E)
1 mV/s	1 A/g	10 mV/s	1 A/g	0.5 A/g	5 mV/s	0.1 A/g	1 A/g
-	0.09	-	32	7.9	0.786	6.08	-
-	-	-	500	200	2810	403	-
-	50% @1500 cycles	94% @8000 cycles	90% @1000 cycles	87.2% @5000 cycles	-	73.9% @1000 cycles	-
[111]	[110]	[109]	[108]	[107]	[106]	[105]	[104]

PANI/CX	PANI	PANI	PANI/LEPC
Aggregated particles	Interconnected nano-bridge and spherical particles	Porous structure	3D network
COP	COP	COP	COP
HCl	Phytic acid	H_2SO_4	-
APS	APS	APS	APS
612 (3E)	523 (3E)	419 (3E)	184 (3E)
0.1 A/g	0.25 A/g	1 A/g	0.5 A/g
13.6	7.75	8.42	3
70.1	45.56	147.2	41.6
61.6% @1500 cycles	88% @10000 cycles	-	74% @1000 cycles
[115]	[114]	[113]	[85]

PANI = Polyaniline

SWCNT = Single wall carbon nanotube

CNF = Carbon nanofiber

CX = Carbon xerogel

LEPC = Low methoxyl group concentration

COP = Chemical oxidative polymerization

EP = Electrochemical polymerization

IP = Interfacial polymerization

3E = Three electrode

SSC = Symmetric supercapacitor

2.3. Metal oxides

Supercapacitor electrodes can be made up of binary transition metal oxides such as $MnFe_2O_4$, $NiCo_2O_4$, $NiFe_2O_4$, etc. as well as single metal oxides such as NiO, CuO, MnO_2, RuO_2, etc. Ruthenium oxides were the subject of intensive research in the 19th and the first decade of the 20th centuries, but the expense prevented their commercialization. Due to the presence of two metal ions, binary transition metal oxides (BTMOs) provide more electroactive sites than single metal oxides (SMOs). Richer redox capability is displayed by BTMOs than SMOs [116].

The structural types of metal ferrites (MFe_2O_4, M = Metal) are either normal spinel type or inverse spinel type. The tetrahedral and octahedral positions, respectively, are occupied by face-centered cubic unit cells of the spinel type M^{2+}-O^{2-} and Fe^{3+}-O^{2-}. In the case of inverse spinel type, unit cells are identical, but trivalent Fe^{3+} cations totally fill tetrahedral sites, and divalent M^{2+} and Fe^{3+} cations evenly occupy octahedral sites. These intriguing structures boost electrical conductivity by allowing electrons to hop between the various valence states of metals in oxygen sites [5,117,118]. A noteworthy observation is that Co_3O_4 (CoO-Co_2O_3) has a typical spinel structure, with Co3+ and Co^{2+} occupying the octahedral and tetrahedral positions, respectively. According to site preference theory, inverse spinels are formed when transition metal oxides like Mn, Ni, or Cu ($MnCo_2O_4$, $NiCo_2O_4$, and $CuCo_2O_4$) are substituted for Co. In these inverse spinels, the foreign cation binds to the octahedral sites while Co takes up both the octahedral and tetrahedral sites. Where the tetrahedron and octahedron share four apexes in this strange configuration, interconnecting interstitial voids

are formed. In addition to providing enough ion diffusing channels, this encourages charge carriers (such as holes or electrons) to jump into the octahedral and tetrahedral sites [119,120].

Aparna et al. (2018) found that the binary metal oxides like $NiFe_2O_4$, $MnFe_2O_4$, $CuFe_2O_4$, $ZnFe_2O_4$ exhibited better electrochemical performances than their individual metal oxides [118]. Haichao et al. (2014) found that $NiCo_2O_4$ had a specific capacitance of 658 F/g at 1 A/g, which was twofold higher than the specific capacitance of NiO and Co_3O_4 [121]. $NiCo_2O_4$ exhibited superior power and energy density than the monometallic oxides due to the involvement of two different metal oxides. Cen et al. (2018) reported that copper-cobalt hybrid oxide exhibited superior electrochemical performances than Cu_2O and CoO, which could be due to the synergistic effects developed after combining the single metal oxides [122]. Loubna et al. (2018) prepared $NiCo_2O_4$, $CuCo_2O_4$, $MnCo_2O_4$, $ZnCo_2O_4$ based supercapacitor electrodes, which gave specific capacitance values of 211 F/g, 285 F/g, 185 F/g, 151 F/g, respectively [123]. Yanying et al. (2017) found that $MnCo_2O_4$ exhibited superior electrochemical behaviour than Co_3O_4 and suggested that presence of two different transition metal oxides in $MnCo_2O_4$ must be providing more electroactive sites for the electrochemical processes [124]. Jianwei et al. (2019) investigated the electrochemical performances of $MnCo_2O_4$, Co_3O_4, Mn_2O_3, and Mn_2O_3/Co_3O_4 based systems, and found that $MnCo_2O_4$ exhibited better electrochemical activities than other systems [125]. Tianfu et al. (2018) fabricated $NiCo_2O_4$, NiO, and Co_3O_4 based supercapacitors [126]. They found that the binary metal oxide based system had a specific capacitance of 429.60 F/g, which was higher than NiO (219.88 F/g) and Co_3O_4 (294.99 F/g).

Table 2.3 summarizes the references of different metal oxides and metal oxide composites as supercapacitor electrodes.

Table 2.3: Electrochemical properties of various metal oxide based systems

Materials	C_{sp} (F/g)	Scan rate or Current density	E_{sp} (Wh/ kg)	P_{sp} (W/ kg)	Cycle life	Ref.
Mn_2O_3-Mn_3O_4-AC	80.8 (SC)	2 mA/cm^2	7.19	980	-	[127]
$NiCr_2O_4$	187 (SC)	0.6 A/g	6.5	3000	80% @2000 cycles	[128]
Mn_3O_4	665.08 (SSC)	-	0.0436	4270	-	[129]
$CoFe_2O_4$	54.5 (SC)	5 A/g	8.51	1020	-	[130]
$ZnCo_2O_4$	1625 (3E)	5 A/g	12.5	800	94% @5000 cycles	[131]
$NiMn_2O_4$	50 (SC)	0.2 mA	15.625	1125	-	[132]
$CuCo_2O_4$	338 (3E)	1 A/g	3.05	22110	-	[133]
$MnFe_2O_4$	24.9 (SC)	-	12.49	830	-	[134]
$ZnMoO_4$	234.75 (SC)	0.5 A/g	20.808	199.44	82% @1600 cycles	[135]
$CoFe_2O_4$	774 (SC)	0.5 mA/cm^2	17	3277	-	[136]

2.4. Composites

Composites of carbon based material, conducting polymer, and metal oxide are found to be more electroactive than the individual systems due to synergistic effect. A comprehensive compilation of the work on composites has been given in table 2.4.

Zou et al. (2018) prepared N-doped graphene/PANI (GMPH7) binary hydrogel [137]. The prepared GMPH7 hydrogel shown the higher specific capacitance 514.3 F/g while 375 F/g for graphene/PANI (GPH7) and 325 F/g for PANI at 1 A/g with 100% retention of its capacitance. Hou et al. (2020) fabricate amine-functionalized graphene/polyaniline (F-rGO/PANI) and mesoporous graphene/polyaniline (PF- rGO/PANI) composite which exhibit high specific capacitance (597 F/g for F-rGO/PANI and 489 F/g for PF- rGO/PANI) at 0.5 A/g current density with 75% and 89% retention respectively [138]. MnO_2/rGO composite prepared using manganese sulfate monohydrate and exhibit capacitance around 759 F/g at 2 A/g current density with 88% capacitance retention for 3500 cycles [139]. Fu and co-workers (2021), presented a facile technique of V_2O_5/graphene composite formation [140]. The high specific capacitance of formed hybrid exhibit 673.2 F/g at 1 A/g current density of V_2O_5/graphene-0.341 (where 0.341 was V_2O_5 mass proportion in composite) with 96.8% retention after 10000 cycle life and excellent energy as well as power density such as 46.8 Wh/kg at 499.4 W/kg, 32.9 Wh/kg at 4746.0 W/kg in 1M Na_2SO_4 electrolyte. GCS@PANI@rGO were synthesized having higher specific capacitance of 446.19 F/g at current density of 2 A/g alongside 93.4% retention after 1000 cycle and even remained 88.7% retention after 5000 charge-discharge cycles, due to the synergic effect of GCS, PANI and rGO [141]. Reduced GO/Fe_3O_4/PANI was synthesized and shown a higher specific capacitance of 610.4 F/g in comparison with rGO/Fe_3O_4 (212.6 F/g) with 87% capacitance because of synergic effect among rGO, Fe_3O_4, PANI as well and absence of agglomeration

of Fe_3O_4 nanoparticles on composite surface [142]. A ternary composite hydrogel PANI/Graphene/Fe_2O_3 was prepared using microwave irradiation method as first step. Furthermore, polymerization process was carried out [143]. The combination of PANI, Graphene, and Fe_2O_3 synergic action displays the high specific capacitance 1124 F/g at 0.25 A/g current density and 923 F/g at 7.5 A/g peak current density with 82.2% retention**.** Another ternary rGO/Au/PANI nanocomposite was synthesized using *Cetraria Islandica L. ach.* extract as a green reducing agent [144]. This hybrid electrode material delivers high specific capacitance of 212.8 F/g at 1 A/g current density and exhibit 86.9% retention after 5000 repeated charge-discharge cycles. The polyaniline based ZnS/rGO/PANI ternary composite exhibits specific capacitance of 1045.3 F/g using three-electrode and 722.0 F/g capacitance using two-electrode system at constant 1 A/g current density [145]. Interestingly PANI based ternary composite holds 76.1% and 160% cycle stability for two-electrode and three-electrode system respectively after 1000 charge-discharge loops. A nanocomposite based on rGO/polypyrrole nanofiber was synthesized via microwave irradiation reduction of GO followed by in-situ polymerization of pyrrole [146]. The higher specific capacitance of 227 F/g at 1 A/g using 1 M H_2SO_4 as a electrolyte and high energy density 38.5 Wh/kg at 500 W/kg power density. Graphene/polypyrrole composite hydrogel prepared with well distribution and cross-linked of PPY on porous graphene structure showed specific capacitance of 295 to 240 F/g at 1 to 10 A/g current density with holds 80% capacitance retention cycle stability after 5000 cycles of charge-discharge [147]. Moreover, ternary hybrid nanocomposite NiO/Graphene/PPY prepared [148]. This hybrid material on $Cu(OH)_2$/Cu foil substrate to formed working electrode for electrochemical analysis. The flaky shape nanocomposite showed high specific capacitance of 970.85 F/g using 6 M KOH

aqueous electrolyte and 66.17 F/g for 1 M $TEABF_4$/AN organic electrolyte. Liang et al. (2021) synthesized Graphene/PPY/Ag hybrid nanocomposite [149]. The synergic nature of these three materials exhibits high areal capacitance 294.2 mF/cm^2 at 1 mA/cm^2 current density with capacitance retention around 80.1% after 5000 loops. The enhanced performance mainly from reversible Ag/Ag^+ redox action and complete wrapping of Ag nanoparticles by PPY on graphene surface. Another novel hybrid nanocomposite PdPGO was synthesized [150]. This exhibit highest capacitance as 595 F/g for PdPGO comparable to 335 F/g of binary PdO/PPY material at 1 A/g current density with 88% cycle stability after 5000 loops. Additionally, Xin et al. (2020) compared the supercapacitor material performance of MoO_3/Graphene aerogel/PPY, MoO_3/GA and PPY, which exhibited the specific capacitance 1788 F/g, 1059 F/g and 379 F/g at 1 A/g [151]. Based on graphene ternary system, the insertion of PbO_2 nanoparticles has been displayed by Abraham and co-workers (2020) into the surface of PPY/rGO for enhanced electrochemical nature of supercapacitor [152].

Ye et al. (2010) synthesized a ternary composite of MnO_2 nanospheres/carbon nanotubes/conducting polymer, which had a specific capacitance higher than the individual systems, i.e., 427 F/g [153]. Xiangjun et al. (2011) reported a ternary system of graphene-polyaniline-carbon nanotube with a specific capacitance of 569 F/g at 0.1 A/g [154]. Yanfang et al. (2012) synthesized a ternary system of PANI-mesoporous carbon-MnO_2. The specific capacitance of PANI, PANI-mesoporous carbon, and ternary composite (12 % MnO_2) were found to be 254 F/g, 587 F/g, and 695 F/g, respectively. He explained that the incorporation of MnO_2 created larger current response in case of ternary composite and therefore, the specific capacitance increased [155]. Xifeng et al. (2012) prepared reduced

graphene oxide-molybdenum oxide-polyaniline based system, which had a higher specific capacitance (553 F/g) than MoO_3/PANI (261 F/g) and RGO/PANI (295 F/g) [156]. Guangxiang et al. (2013) fabricated sulfonated graphene-MnO_2-polyaniline based supercapacitors. They found that the specific capacitance of the ternary system (276 F/g at 1 A/g) was higher than that of MnO_2/PANI (228 F/g). They reported less IR drop (potential drop) in case of ternary material than MnO_2/PANI, and concluded that the internal resistance decreased significantly by introducing sulfonated graphene, and therefore, reduced the energy wastage during charge-discharge process [11]. Ke et al. (2014) found that Fe_3O_4/CNT/PANI composite exhibited 260 F/g of specific capacitance, which was higher than the capacitances obtained for Fe_3O_4/CNT (208 F/g) and Fe_3O_4 (128 F/g). They found that PANI with 8 weight percent provided higher specific capacitance than PANI with 6 and 10 weight percent. The decrease in specific capacitance with increase in PANI content could be due to the agglomeration of the particles of PANI, which would have affected the interconnection between PANI, CNT, and Fe_3O_4 and diminished the synergistic effect [157]. Kalimuthu et al. (2014) reported that the specific capacitance of $MnFe_2O_4$-graphene-PANI (MGP) was 338 F/g at 0.5 mA/cm^2 which was 10-fold of pristine $MnFe_2O_4$ electrode (32 F/g). They suggested that the distinctively superior electrochemical properties of the ternary system were likely due to the reduction of diffusion path and internal resistance via synergistic effect. They also found that the specific capacitance and energy density were increasing with increase in graphene content for binary $MnFe_2O_4$-graphene. But, when PANI weight percentage varied from 5 to 15 % (MGP5-MGP15), the specific capacitance first increased then decreased. MGP-5, MGP-10, and MGP-15 had specific capacitances of 244 F/g, 247 F/g, and 240 F/g, respectively at 5 mV/s. They suggested that at low weight % of

PANI, EDLC mechanism contributed to the capacitance (mostly). When the concentration of PANI increased, the redox reactions predominantly enhanced the capacitance [158]. Debasis et al. (2014) studied the electrochemical behaviours of RGO, $Ni(OH)_2$, and PANI. They reported that RGO-$Ni(OH)_2$ and $Ni(OH)_2$ had specific capacitance of 359 F/g and 238 F/g, respectively. The ternary system displayed an increased specific capacitance of 514 F/g at 2 A/g. They concluded that introduction of PANI increased the pseudocapacitive behaviour and electrical conductivity of the ternary composite [159]. Kalimuthu et al. (2015) reported a ternary hybrid composite system of $MnFe_2O_4$/graphene/polyaniline. They found that the specific capacitance of ternary system was 7.5 times than $MnFe_2O_4$. They mentioned that the outstanding electrochemical properties of ternary composite could be due to the low internal resistance, reduced diffusion length, large active sites, low diffusive resistance and synergistic effect developed between the constituents [160]. Hamid et al. (2015) noticed that carbon black-graphite-MnO_2 based ternary system recorded higher current response than individual systems. The enhanced current could be the result of synergistic effect between CB, graphite, and MnO_2 [161]. Huailong et al. (2015) reported that RGO-MnO_2-PANI composite with PANI, MnO_2, and RGO of 10.6 %, 36.7 %, and 52.7 %, respectively had the highest specific capacitance of 636.5 F/g. They also reported that when PANI was increased to 17.3 %, the capacitance decreased significantly. Excessive amount of PANI nanorods might be blocking the active sites and inevitably weakening the electrochemical activities. They described various advantages of the ternary system. (i) Embedment of PANI with MnO_2 increased the electroactive sites for reversible and fast faradaic transitions along with the creation of abundant open channels for effortless penetration of the mobile electrolyte ions into the electrodes. (ii) MnO_2/PANI strongly adhered to RGO and avoided any addition

of conductive fillers during electrode fabrication. This increased the utilization of electroactive materials, and the capacitance and rate capability were boosted [162]. Anukul et al. (2017) evaluated the electrochemical performances of PANI-CNT-MoS_2 and reported a specific capacitance of 350 F/g at 1 A/g for 5% MoS_2, which was higher than the individuals. When MoS_2 was 2.5% and 10% in the ternary composite, they observed lesser specific capacitance of 320 F/g and 240 F/g, respectively. 2.5% of MoS_2 was not much effective to overcome pore blockages of PANI due to agglomeration of CNT and therefore, could not surmount ion exchange hindrance. However, MoS_2 with 5 weight percentage optimized the available surface area and ion exchange took place seamlessly between PANI and the electrolyte, and in turn increased the capacitance. With increase in MoS_2 weight percentage to 10%, the specific capacitance decreased, which could be due to the active pore blockage by surplus amount of MoS_2 particles. More MoS_2 could be tightly packed on the surface of PANI, thereby inhibiting proper ion exchange between PANI and the electrolyte [163]. Yu et al. (2018) synthesized a ternary composite of polyaniline/graphene oxide/copper. They reported that the conductivity increased with the increase in mass fraction of GO/Cu from 0 to 50%, but the specific capacitance increased till 10%, then started decreasing. When the mass fraction increased, the electrical double layer capacitance of graphene dominated, as a result the capacitance decreased. PANI/GO/Cu with GO/Cu of 10 weight % had the highest specific capacitance of 558 F/g. Pure GO and PANI had C_{sp} of 180 F/g and 289 F/g, respectively [164]. Ozan et al. (2021) fabricated graphene oxide-TiO_2-PANI based system with different ratio of the constituents. The specific capacitance was found to be optimum at the ratio of 1:5:4 (GO:TiO_2:PANI), i.e., 692.87 F/g at 2 mV/s. The proportion of 1:5:3 provided the highest energy density of 7.79 Wh/kg at 20 mA and 8910

W/kg of power density at 50 mA. The ratio of 1:5:2 had the lowest impedance of 87.4 Ω [165]. Akshaya et al. (2021) synthesized polyaniline (P), graphene (N), $CuCr_2O_4$ (C) based ternary system having weight ratio of 75:20:5 (PNC-75). PNC-75 had the highest specific capacitance of 572.4 F/g, whereas pure PANI, PN, and PC exhibited specific capacitance values of 320.7 F/g, 309 F/g, and 194.4 F/g, respectively. The specific capacitance kept on increasing when PANI loading was from 55 to 75%, but it started decreasing when PANI weight percentage exceeded 75% (for PNC-85). They suggested that the downward trend of C_{sp} could be the result of the suppression of EDLC nature of graphene due to more pseudocapacitive contribution originated from PANI. Another reason could be the staggered movement of electrolyte ions through the pores of PANI, which created hindrance to the electrochemical activities. The obtained charge transfer resistances for PANI, PN, PC, and PNC-75 were 1.498 Ω, 1.28 Ω, 1.33 Ω, and 1.23 Ω, respectively [166]. Shatrudhan et al. (2021) fabricated a symmetric supercapacitor of PANI-RGO-ZnO. The amount of aniline:ZnO was varied as 1:2 and 2:1 by keeping RGO constant. They found that PANI-RGO-ZnO-2:1 based system exhibited the highest specific capacitance of 125 F/g, whereas PANI-RGO and PANI-RGO-ZnO-1:2 based devices had 63 F/g and 61 F/g of specific capacitance, respectively. The ternary system based symmetric supercapacitor device had specific energy and power of 5.61 Wh/kg and 14.68 W/kg at 0.05 A/g. So, it is necessary to know the optimized weight ratio of the constituents at which they can provide outstanding electrochemical activities [167].

Table 2.4: Electrochemical properties of various composite hybrid supercapacitor electrodes and devices

Materials	C_{sp} (F/g)	Scan rate or Current density	E_{sp} (Wh/ kg)	P_{sp} (W/ kg)	Cycle life	Ref.
Graphene-PANI-TiO_2	403.2 (3E)	2 A/g	-	-	80% @1000 cycles	[168]
Graphene/PANI@MnO_2	695 (3E)	4 A/g	2	31200	-	[169]
Graphene/PANI/MoS_2	142.3 (SSC)	0.98 A/g	2.65	119.21	98.11% @500 cycles	[170]
PANI@Fe_3O_4@CFs	245.5 (3E)	0.5 A/g	78.6	1047.5	82.44% @1000 cycles	[171]
PPY-PB-CB	163.7 (SC)	1 mV/s	18.1	10780	98.35% @2000 cycles	[172]
RGO-PANI-Fe_2O_3	605.2 (3E)	0.5 A/g	-	-	90.6% @5000 cycles	[173]
Co_3O_4/PANI/Graphene	476 (3E)	2 A/g	33.5	800	-	[174]
MWCNTs/$FeNi_3$/PANI	398.1 (3E)	0.5 A/g	9.1	500	80.9% @2000 cycles	[175]
N-doped Graphene/$NiFe_2O_4$/PANI	667 (3E)	0.1 A/g	23.2	27.7	90% @1000 0 cycles	[176]
MnO_2/PANI/RGO	571 (3E)	1 A/g	-	-	96.7% @1000 0 cycles	[177]

MnS/GO/PANI	207.13 (SC)	10 mV/s	18.41	-	81.6% @5000 cycles	[178]
RGO-Au@PANI	212.8 (SC)	1 A/g	7.52	126.5	86.9% @5000 cycles	[144]

CF = Carbon fiber

PPY = Polypyrrole

PB = Prussian blue

2.5. Benefits of the ternary composite system

Charge accumulation properties can be found in carbon-based materials, conducting polymers, and metal oxides. Contrarily, carbon materials and conducting polymers readily engage in electrochemical processes due to their polar nature and high wettability, in contrast to the inner active sites of metal oxides, which have limited anion/cation diffusion due to their compact size [179]. Carbon-based compounds and conducting polymers are typically used to prevent the agglomerations of metal oxides. Fewer agglomeration results in pores of a bigger size, which speeds up ionic transport and enhances electrochemical activity. Due to hydrolysis and structural change, it is discovered that conducting polymers like polyaniline has lower capacitance retention [180]. Unwanted byproducts that reduce conductivity and stability are produced as a result of hydrolysis. The polymer's structural integrity could be harmed, and the active surface area could be reduced. They all work in concert to slow down the electrochemical kinetics, decrease the electroactive surface area, and disrupt the electrode/electrolyte interaction. So, the use of ternary composite as electrodes for supercapacitor applications can negate and overcome the individual drawbacks and the system will provide powerful performance.

2.6. Research Gap

Based on the literature survey, the following research gaps were identified:

(a) There are few researches on AB_2O_4 (A and B are metals, and O stands for oxygen) type metal oxides.

(b) Graphene oxide (GO) is used as a carbon material and conductive filler in supercapacitor electrodes, but it increases the overall resistance. Very few attempts have been made to take it as a source of carbon material in fabricating supercapacitor electrodes.

(c) PTSA (Para toluene sulfonic acid) is a very good dopant. But there is not enough research over its effect on the electrochemical properties of polyaniline.

(d) Few researches have been performed on the synthesis of ternary composite based supercapacitor electrodes.

(e) Still, energy density remains a major setback for supercapacitors.

2.7. Objectives

The current research was conducted with the following objectives;

(a) Use GO as a component for the composite material synthesis to avoid surplus charge transfer resistance.

(b) To explore GO-PANI-$CuCo_2O_4$, GO-PANI-$CuFe_2O_4$, GO-PANI-$CoFe_2O_4$ based ternary composites, which have never been studied.

(c) To find the best material on the basis of electrochemical performances of the individual, binary, and ternary systems.

(d) Fabricating supercapacitors with enhanced specific capacitance, specific energy, specific power, and prolonged cycle life.